Fast spin ±2 spherical harmonics transforms and application in cosmology

Y. Wiaux [a,*], L. Jacques [b], P. Vandergheynst [a]

[a] *Signal Processing Institute, Ecole Polytechnique Fédérale de Lausanne (EPFL), CH-1015 Lausanne, Switzerland*

[b] *Communications and Remote Sensing Laboratory, Université catholique de Louvain (UCL), B-1348 Louvain-la-Neuve, Belgium*

Abstract

A fast and exact algorithm is developed for the spin ±2 spherical harmonics transforms on equi-angular pixelizations on the sphere. It is based on the Driscoll and Healy fast scalar spherical harmonics transform. The theoretical exactness of the transform relies on a sampling theorem. The associated asymptotic complexity is of order $\mathcal{O}(L^2 \log_2^2 L)$, where $2L$ stands for the square-root of the number of sampling points on the sphere, also setting a band limit L for the spin ±2 functions considered. The algorithm is presented as an alternative to existing fast algorithms with an asymptotic complexity of order $\mathcal{O}(L^3)$ on other pixelizations. We also illustrate these generic developments through their application in cosmology, for the analysis of the cosmic microwave background (CMB) polarization data.

Key words: computational methods, data analysis, cosmology, cosmic microwave background

1 Introduction

In the last few years, the analysis of the temperature anisotropies of the cosmic microwave background (CMB), together with other cosmological observations, has allowed the definition of a precise concordance cosmological model. These observations culminated with the release of the three-year data of the Wilkinson Microwave Anisotropy Probe (WMAP) satellite experiment. The

* Corresponding author.
Email address: yves.wiaux@epfl.ch (Y. Wiaux).

cosmological parameters are now determined with an unprecedented precision of the order of several percent [1,2,3,4]. In the concordance model, the CMB originates from quantum energy fluctuations defined in a primordial era of inflation. These tiny fluctuations are Gaussian in first approximation. The cosmological principle of homogeneity and isotropy of the universe is also assumed. The observed radiation is therefore understood as a unique realization of a Gaussian and stationary (*i.e.* homogeneous and isotropic) random process on the sphere, which may be completely characterized from its two-point correlation functions, or the corresponding angular power spectra.

The present concordance values of the cosmological parameters are obtained through a best fit of the theoretical temperature angular power spectrum of the CMB with the experimental data. Beyond temperature anisotropies, *i.e.* intensity anisotropies, a polarization of the CMB is also present which constitutes a complementary source of information for cosmology. This polarization is produced through Thomson scattering at the epoch of recombination. The degree of polarization of the CMB is expected to be of the order of 10 percent of the temperature anisotropies at small scales, and lower at large scales. As Thomson scattering only produces linearly polarized light, the CMB radiation is completely described by its temperature T, and its linear polarization Stokes parameters Q and U [5,6,7,8,9,10]. First polarization measurements were recently obtained, notably by the WMAP experiment [11]. Future CMB experiments such as the Planck surveyor satellite experiment will allow a deeper probe of the temperature and polarization spectra, thanks to improved sensitivity and resolution on the whole sky.

From the mathematical point of view, the observable temperature T is a scalar function on the sphere, *i.e.* invariant under local rotations in the plane tangent to the sphere at each point. The associated invariant TT angular power spectrum results from the decomposition of the temperature in scalar spherical harmonics. But the observable polarization Stokes parameters Q and U transform as the components of a transverse, symmetric, and traceless rank 2 tensor under local rotations. However, scalar electric E and magnetic B polarization components may equivalently be defined from the parameters Q and U. The associated invariant EE and BB polarization angular power spectra, and the cross-correlation TE spectrum result from the decomposition of the combinations $Q \pm iU$ in spin ± 2 spherical harmonics on the sphere [6]. From the numerical point of view, the asymptotic complexity associated with a naive quadrature based on the definition of the scalar and spin ± 2 spherical harmonics transforms is of order $\mathcal{O}(L^4)$, where L roughly identifies the square-root of the number of sampling points on the sphere. Corresponding computation times for the analysis of megapixels all-sky maps such as those of the ongoing WMAP or the forthcoming Planck experiments are of the order of days. Fast and precise computation methods for the scalar and spin ± 2 spherical harmonics transforms of functions on the sphere are therefore needed.

Beyond cosmology, an algorithm for the spin ± 2 spherical harmonics transforms will find application in the spectral analysis of arbitrary spin ± 2 signals on the sphere, components of transverse, symmetric, and traceless rank 2 tensor fields under local rotations.

In the present work we develop a fast algorithm for the spin ± 2 spherical harmonics transforms of band-limited functions on the sphere. It is based on an existing fast algorithm for the scalar spherical harmonics transform. It is defined on $2L \times 2L$ equi-angular pixelizations in spherical coordinates (θ, φ) on the sphere. The algorithm is theoretically exact thanks to the existence of a sampling theorem. The associated asymptotic complexity is of order $\mathcal{O}(L^2 \log_2^2 L)$. Corresponding computation times for megapixels maps are reduced to seconds. The algorithm is presented as an alternative to existing fast algorithms with an asymptotic complexity of order $\mathcal{O}(L^3)$ on other pixelizations which are widely used in the context of astrophysics and cosmology.

In § 2, we recall the notion of spin n functions on the sphere. In § 3, we define and implement a fast and exact algorithm with complexity $\mathcal{O}(L^2 \log_2^2 L)$ for the spin ± 2 spherical harmonics transforms on equi-angular pixelizations. In § 4, we illustrate the interest of our algorithm in the context of the analysis of CMB polarization data. We finally briefly conclude in § 5.

2 Spin n functions on the sphere

In this section, we discuss standard harmonic analysis on the sphere and on the rotation group $SO(3)$. We also discuss the notion of spin n functions on the sphere and their decomposition in a basis of spin-weighted spherical harmonics of spin n.

2.1 Standard harmonic analysis

Let the function $G(\omega)$ be a square-integrable function in $L^2(S^2, d\Omega)$ on the unit sphere S^2. The spherical coordinates of a point on the unit sphere, defined in the right-handed Cartesian coordinate system $(o, o\hat{x}, o\hat{y}, o\hat{z})$ centered on the sphere, read as $\omega = (\theta, \varphi)$. The angle $\theta \in [0, \pi]$ is the polar angle, or co-latitude. The angle $\varphi \in [0, 2\pi[$ is the azimuthal angle, or longitude. The invariant measure on the sphere reads $d\Omega = d\cos\theta d\varphi$. The standard scalar spherical harmonics $Y_{lm}(\omega)$, with $l \in \mathbb{N}$, $m \in \mathbb{Z}$, and $|m| \leq l$, form an orthonormal basis for the decomposition of functions in $L^2(S^2, d\Omega)$ on the sphere [12]. They are explicitly given in a factorized form in terms of the associated Legendre

polynomials $P_l^m(\cos\theta)$ and the complex exponentials $e^{im\varphi}$ as

$$Y_{lm}(\theta,\varphi) = \left[\frac{2l+1}{4\pi}\frac{(l-m)!}{(l+m)!}\right]^{1/2} P_l^m(\cos\theta)\, e^{im\varphi}. \quad (1)$$

This corresponds to the choice of Condon-Shortley phase $(-1)^m$ for the spherical harmonics, ensuring the relation $(-1)^m Y_{lm}^*(\omega) = Y_{l(-m)}(\omega)$. This phase is here included in the definition of the associated Legendre polynomials [13,12]. Another convention [14] explicitly transfers it to the spherical harmonics. Any function $G(\omega)$ on the sphere is thus uniquely given as a linear combination of scalar spherical harmonics: $G(\omega) = \sum_{l\in\mathbb{N}}\sum_{|m|\leq l}\widehat{G}_{lm}Y_{lm}(\omega)$ (inverse transform), for the scalar spherical harmonics coefficients $\widehat{G}_{lm} = \int_{S^2} d\Omega\, Y_{lm}^*(\omega)G(\omega)$ (direct transform), with $|m|\leq l$.

Let now $G(\rho)$ be a square-integrable function in $L^2(SO(3),d\rho)$ on the group $SO(3)$ of three-dimensional rotations. Any rotation $\rho\in SO(3)$ may be explicitly given in the Euler angles parametrization as $\rho=(\varphi,\theta,\chi)$, describing successive rotations by the Euler angles $\chi\in[0,2\pi[$, $\theta\in[0,\pi]$, and $\varphi\in[0,2\pi[$, around the axes of coordinate $o\hat{z}$, $o\hat{y}$, and $o\hat{z}$ respectively. The invariant measure on the rotation group reads $d\rho = d\varphi d\cos\theta d\chi$. The Wigner D-functions $D_{mn}^l(\rho)$, with $l\in\mathbb{N}$, $m,n\in\mathbb{Z}$, and $|m|,|n|\leq l$, are the matrix elements of the irreducible unitary representations of weight l of the rotation group $SO(3)$, in $L^2(SO(3),d\rho)$. By the Peter-Weyl theorem on compact groups, the matrix elements D_{mn}^{l*} also form an orthogonal basis in $L^2(SO(3),d\rho)$ [12]. They are explicitly given in a factorized form in terms of the real Wigner d-functions $d_{mn}^l(\theta)$ and the complex exponentials $e^{-im\varphi}$ and $e^{-in\chi}$ as

$$D_{mn}^l(\varphi,\theta,\chi) = e^{-im\varphi}d_{mn}^l(\theta)\, e^{-in\chi}. \quad (2)$$

Any function $G(\rho)$ in $L^2(SO(3),d\rho)$ is thus uniquely given as a linear combination of Wigner D-functions : $G(\rho) = \sum_{l\in\mathbb{N}}(2l+1)/8\pi^2\sum_{|m|,|n|\leq l}\widehat{G}_{mn}^l D_{mn}^{l*}(\rho)$ (inverse transform), with $|m|,|n|\leq l$ and where $\widehat{G}_{mn}^l = \int_{SO(3)} d\rho\, D_{mn}^l(\rho)G(\rho)$ (direct transform) stands for the with Wigner D-functions coefficients.

2.2 Spin n functions

Let us define a spin n square-integrable function ${}_nG(\omega)$ in $L^2(S^2,d\Omega)$ on the sphere. The Euler angles (φ,θ,χ) associated with a general rotation ρ in three dimensions may also be interpreted in the reverse order as successive rotations by φ around $o\hat{z}$, θ around $o\hat{y}'$, and χ around $o\hat{z}''$, where the axes $o\hat{y}'\equiv o\hat{y}'(\varphi)$ and $o\hat{z}''\equiv o\hat{z}''(\varphi,\theta)$ are respectively obtained by the first and second rotations of the coordinate system by φ and θ [14]. The local rotations of the basis vectors in the plane tangent to the sphere at $\omega=(\theta,\varphi)$ are rotations around $o\hat{z}''$, therefore associated with the third Euler angle χ. Spin n functions on the

sphere ${}_nG(\omega)$, with $n \in \mathbb{Z}$, are defined relatively to their behavior under the corresponding right-handed rotations by χ_0 as [15,16,17]:

$$ {}_nG'(\omega) = e^{-in\chi_0}\ {}_nG(\omega). \tag{3} $$

The standard square-integrable functions on the sphere considered above are spin 0 or scalar functions. Let us emphasize that the rotations considered are local transformations on the sphere around the axis $o\hat{z}'' \equiv o\hat{z}''(\varphi,\theta)$, affecting the coordinate χ in the tangent plane independently at each point $\omega = (\theta,\varphi)$, and according to $\chi' = \chi - \chi_0$. They are to be clearly distinguished from the global rotations by χ around $o\hat{z}$ associated with the alternative Euler angles interpretation, which affect the coordinates of the points $\omega = (\theta,\varphi)$ on the sphere. Our sign convention in the exponential is coherent with the definition (4) below for the spin-weighted spherical harmonics of spin n. It is opposite to the original definition [15], while equivalent to recent notations used in the context of the CMB analysis [6,10].

Recalling the factorized form (2), spin functions are equivalently defined as the evaluation at $\chi = 0$ of any function in $L^2(SO(3), d\rho)$ resulting from an expansion for fixed index n in the Wigner D-functions $D^l_{mn}(\varphi,\theta,\chi)$. The functions $D^l_{mn}(\varphi,\theta,0)$ or $D^{l*}_{m(-n)}(\varphi,\theta,0)$ thus naturally define for each n an orthogonal basis for the expansion of spin n functions in $L^2(S^2, d\Omega)$ on the sphere. After normalization in $L^2(S^2, d\Omega)$, the spin-weighted spherical harmonics of spin n are given in a factorized form in terms of the real Wigner d-functions $d^l_{mn}(\theta)$ and the complex exponentials $e^{im\varphi}$ as

$$ {}_nY_{lm}(\theta,\varphi) = (-1)^n \sqrt{\frac{2l+1}{4\pi}} d^l_{m(-n)}(\theta)\, e^{im\varphi}, \tag{4} $$

with $l \in \mathbb{N}$, $l \geq |n|$, and $m \in \mathbb{Z}$, $|m| \leq l$. In particular, the symmetry properties of the Wigner d-functions [12] imply the generalized symmetry relation $(-1)^{n+m}\ {}_nY^*_{lm}(\omega) = {}_{-n}Y_{l(-m)}(\omega)$. The spin 0 spherical harmonics explicitly identify with the standard scalar spherical harmonics for the decomposition of scalar functions: ${}_0Y_{lm}(\omega) = Y_{lm}(\omega)$, through the relation $d^l_{m0}(\theta) = [(l-m)!/(l+m)!]^{1/2} P^m_l(\cos\theta)$. Any spin n function ${}_nG(\omega)$ on the sphere is thus uniquely given as a linear combination of spin n spherical harmonics : ${}_nG(\omega) = \sum_{l\in\mathbb{N}} \sum_{|m|\leq l}\ {}_n\widehat{G}_{lm}\ {}_nY_{lm}(\omega)$ (inverse transform), for the spin-weighted spherical harmonics coefficients ${}_n\widehat{G}_{lm} = \int_{S^2} d\Omega\ {}_nY^*_{lm}(\omega) G(\omega)$ (direct transform), with $l \geq |n|$, and $|m| \leq l$.

Finally, spin $n \pm 1$ functions may be defined from spin n functions through the action of the so-called spin raising and lowering operators [15,16]. The action of the spin raising $\eth$ and lowering $\bar{\eth}$ operators on a spin n function ${}_nG$, giving spin $n+1$ and $n-1$ functions respectively, is defined as

$$[\eth\ {}_nG](\theta,\varphi) = \left[-\sin^n\theta\left(\frac{\partial}{\partial\theta} + \frac{i}{\sin\theta}\frac{\partial}{\partial\varphi}\right)\sin^{-n}\theta\ {}_nG\right](\theta,\varphi) \tag{5}$$

and

$$\left[\bar{\eth}\ {}_nG\right](\theta,\varphi) = \left[-\sin^{-n}\theta\left(\frac{\partial}{\partial\theta} - \frac{i}{\sin\theta}\frac{\partial}{\partial\varphi}\right)\sin^{n}\theta\ {}_nG\right](\theta,\varphi), \tag{6}$$

with, under rotation by χ_0 in the tangent plane at $\omega = (\theta,\varphi)$: $[\eth\ {}_nG]'(\omega) = e^{-i(n+1)\chi_0}[\eth\ {}_nG](\omega)$ and $[\bar{\eth}\ {}_nG]'(\omega) = e^{-i(n-1)\chi_0}[\bar{\eth}\ {}_nG](\omega)$. In these terms, the spin-weighted spherical harmonics of spin n are related to spin-weighted spherical harmonics of spins $n+1$ and $n-1$ through the following relations:

$$[\eth\ {}_nY_{lm}](\omega) = [(l-n)(l+n+1)]^{1/2}\ {}_{n+1}Y_{lm}(\omega) \tag{7}$$

and

$$\left[\bar{\eth}\ {}_nY_{lm}\right](\omega) = -[(l+n)(l-n+1)]^{1/2}\ {}_{n-1}Y_{lm}(\omega), \tag{8}$$

also implying

$$\left[\bar{\eth}\eth\ {}_nY_{lm}\right](\omega) = -(l-n)(l+n+1)\ {}_nY_{lm}(\omega). \tag{9}$$

The corresponding direct relation between the spin-weighted spherical harmonics of spin n and scalar spherical harmonics reads:

$${}_nY_{lm}(\omega) = \left[\frac{(l-n)!}{(l+n)!}\right]^{1/2}[\eth^n Y_{lm}](\omega), \tag{10}$$

for $0 \leq n \leq l$, and

$${}_nY_{lm}(\omega) = \left[\frac{(l+n)!}{(l-n)!}\right]^{1/2}(-1)^n\left[\bar{\eth}^{-n}Y_{lm}\right](\omega), \tag{11}$$

for $-l \leq n \leq 0$.

These relations between spin-weighted and scalar spherical harmonics are explicitly used in § 3 for the development of a fast direct spin ± 2 spherical harmonics transforms algorithm.

3 Fast spin ± 2 transforms algorithm

In this section, we define and implement a fast and exact algorithm for the computation of the spin ± 2 spherical harmonics transforms of band-limited functions on equi-angular pixelizations on the sphere. The algorithm is based on the relations between spin-weighted and scalar spherical harmonics established in the previous section.

3.1 Pixelizations and existing $\mathcal{O}(L^3)$ algorithms

A $2L \times 2L$ equi-angular pixelization in spherical coordinates (θ, φ) is defined on points $\omega_{ij} = (\theta_i, \varphi_j)$ for $0 \leq i, j \leq 2L-1$, with a uniform discretization of the coordinates: $\Delta\theta = \theta_{i+1} - \theta_i = \pi/2L$ and $\Delta\varphi = \varphi_{j+1} - \varphi_j = 2\pi/2L$. The specific choice $\theta_0 = \pi/4L$, and $\varphi_0 = 0$ is considered in the following implementations. It gives $\theta_i = (2i+1)\pi/4L$ and $\varphi_j = 2j\pi/2L$, and excludes the poles of the sampling, which can be convenient for numerical reasons. The pixels centers are identified with the sampling points ω_{ij} defined here above. The pixels edges are identified by meridians shifted by $\Delta\theta/2 = \pi/4L$, and parallels shifted by $\Delta\varphi/2 = 2\pi/4L$ relative to ω_{ij}. The poles therefore appear as pixels corners. In the next paragraphs, we analyze the properties of equi-angular pixelizations which are of interest in the implementation of scalar and spin ± 2 spherical harmonics transforms. These properties are discussed in comparison with the HEALPix pixelization [1] (Hierarchical Equal Area iso-Latitude Pixelization) [18], and the GLESP pixelization [2] (Gauss-Legendre Sky Pixelization) [19,20], which are widely used in astrophysics and cosmology.

Firstly, we discuss the asymptotic complexity for the computation of scalar and spin ± 2 spherical harmonics transforms. Let us consider band-limited functions ${}_nG(\omega)$ on the sphere with band limit L, defined through the following condition on their scalar ($n = 0$) or spin-weighted ($n \neq 0$) spherical harmonics coefficients: ${}_n\widehat{G}_{lm} = 0$ for $l \geq L$. For a signal with band-limit L, the *a priori* complexity associated with the naive computation of the direct scalar spherical harmonics transform integral on the sphere through simple discretization, *i.e.* a quadrature, for all (l, m) with $|m| \leq l < L$, is naturally of order $\mathcal{O}(L^4)$. And the *a priori* complexity associated with the naive computation of the direct spin ± 2 spherical harmonics transforms integrals on the sphere through simple quadrature, for all (l, m) with $l \geq 2$, and $|m| \leq l < L$, is also naturally of order $\mathcal{O}(L^4)$. The same complexity naturally applies to the corresponding inverse scalar or spin ± 2 transforms. We consider fine samplings corresponding to megapixels maps on the sphere. In particular, the WMAP experiment currently provides all-sky maps of around three megapixels. For such a fine sampling defining a band limit around $L \simeq 10^3$, the typical computation time for $(2L)^2$ multiplications and $(2L)^2$ additions of double-precision numbers is of order of 0.03 seconds on a standard 2.2 GHz Intel Pentium Xeon CPU. We take this value as a fair estimation of the computation time required for one integration for given (l, m), or one summation for given (θ, φ), with an associated $\mathcal{O}(L^2)$ asymptotic complexity. Consequently, scalar or spin ± 2 spherical harmonics transforms, with an asymptotic complexity of order $\mathcal{O}(L^4)$, typically take several days at that band limit $L \simeq 10^3$ on a single

[1] http://healpix.jpl.nasa.gov/
[2] http://www.glesp.nbi.dk/

standard computer. Considering the analysis of a large number of signals or simulations may become difficultly affordable in terms of computation times, *a fortiori* in the perspective of forthcoming experiments with improved resolution on the sky, such as the Planck satellite experiment which will release all-sky maps of around fifty megapixels.

The development of a fast and exact algorithm is therefore of great interest for the CMB analysis. The technique of separation of variables in the scalar or spin ± 2 spherical harmonics into the associated Legendre polynomials $P_l^m(\cos\theta)$ or the Wigner d-functions $d^l_{m2}(\theta)$, and the complex exponentials $e^{im\varphi}$ allows to decompose the transform as successive transforms in φ and θ [21,22]. It naturally reduces the asymptotic complexity for the direct and inverse scalar and spin ± 2 spherical harmonics transforms to $\mathcal{O}(L^3)$. It can be implemented on any iso-latitude pixelization. Many pixelization schemes have been considered on the sphere which satisfy this requirement. It is the case for the equi-angular, HEALPix, and GLESP pixelizations. The algorithms existing on HEALPix or GLESP pixelizations are indeed based on this technique. As discussed in the next subsection, the asymptotic complexity may be further reduced on equi-angular pixelizations.

Secondly, we discuss the precision of the computation. A sampling theorem exists on equi-angular pixelizations on the sphere, which represents a generalization of the Nyquist-Shannon theorem on the line. The sampling theorem states that the scalar spherical harmonics coefficients of a band-limited function on the sphere may be computed exactly up to a band limit L, through a $2L \times 2L$ equi-angular sampling, as a finite weighted sum, *i.e.* a quadrature, of the sampled values of that function [23]. The weights are defined from the structure of the Legendre polynomials $P_l(\cos\theta)$ on the interval $[0, \pi]$. A Gaussian quadrature rule for the exact computation of spherical harmonics coefficients of band-limited functions also exists on GLESP pixelizations. The HEALPix implementation of the scalar and spin ± 2 spherical harmonics transforms achieves a very good precision thanks to an iteration process, but it is only approximate from the theoretical point of view as no sampling theorem is established on such pixelizations.

Thirdly, we comment on the notion of pixel window function. On equi-angular pixelizations, the area A of pixels varies considerably with the co-latitude, from small pixels close to the poles, to larger pixels around the equator: $A(\omega_{ij}) \simeq \sin\theta_i \Delta\theta \Delta\varphi$. This is a major difference with the HEALPix pixelization which defines equal-area pixels, or the GLESP pixelization which defines nearly equal-area pixels. The constant area of pixels is an important property allowing the definition of a pixel window function associated to a given pixelization at a given resolution. The main interest of this concept is to apply a low-pass filtering to the signal, implementing the fact that the pixelized signal is smoothed by integration over the pixel area. The corresponding window

function depends on the pixelization structure and resolution. The procedure of pixelization is approximated to a correlation of the signal with an axisymmetric beam, and therefore strongly relies on the assumption of equal-area pixels. We do not consider here the generalization of this concept on equi-angular pixelizations, where the pixel area varies drastically over the surface of the sphere. We only consider signals with band limit L on a $2L \times 2L$ equi-angular sampling. In this case, for an application such as the downsampling, the spherical harmonics coefficients of a signal can be computed exactly thanks to the sampling theorem, and truncated at the desired band limit. In that respect at least, the use of the pixel window function can be avoided.

Let us finally emphasize that each pixelization scheme (equi-angular, HEALPix, GLESP, ...) may provide specific advantages. The new algorithm proposed in the next subsection on equi-angular pixelizations is exact and has an asymptotic complexity of order $\mathcal{O}(L^2 \log_2^2 L)$. But pixelizations with equal-area pixels represent an advantage when dealing with noisy data [18]. Our algorithm is therefore to be understood as a simple alternative to the existing algorithms. A more detailed comparison of the various algorithms is out of the scope of the present work.

3.2 New exact $\mathcal{O}(L^2 \log_2^2 L)$ algorithm

We recall the following derivative relation on the associated Legendre polynomials [13],

$$\left[\frac{\partial}{\partial\theta} P_l^m\right](\cos\theta) = l\cot\theta P_l^m(\cos\theta) - \frac{l+m}{\sin\theta} P_{l-1}^m(\cos\theta), \tag{12}$$

under the convention that P_l^m is defined to be zero for $l < |m|$. Through this relation, the derivative relations (10) and (11) between the spin ± 2 spherical harmonics ${}_{\pm 2}Y_{lm}$ and the scalar spherical harmonics Y_{lm} may be turned into a simple expression of ${}_{\pm 2}Y_{lm}$ as linear combinations without derivatives of Y_{lm}, $Y_{(l-1)m}$, and $Y_{(l-2)m}$. Notice that the same recurrence procedure is used in a different context in [24], in order to express spin n spherical harmonics ${}_nY_{lm}$, for any n with $0 \leq |n| \leq l$, as linear combinations of scalar spherical harmonics. Through the recurrence relation on l satisfied by the associated Legendre polynomials of given m,

$$(l-m) P_l^m(\cos\theta) = (2l-1)\cos\theta P_{l-1}^m(\cos\theta) - (l+m-1) P_{l-2}^m(\cos\theta), \tag{13}$$

the $Y_{(l-2)m}$ term in the quoted linear combination for ${}_{\pm 2}Y_{lm}$ may be cancelled. We finally obtain the following expression of ${}_{\pm 2}Y_{lm}$ as a linear combination of

the scalar spherical harmonics Y_{lm} and $Y_{(l-1)m}$:

$$ {}_{\pm 2}Y_{lm}(\theta,\varphi) = \left[\frac{(l-2)!}{(l+2)!}\right]^{1/2} \left[\alpha^{\pm}_{(lm)}(\theta)\, Y_{lm}(\theta,\varphi) + \beta^{\pm}_{(lm)}(\theta)\, Y_{(l-1)m}(\theta,\varphi)\right], \tag{14} $$

for $l \geq 2$ and $|m| \leq l$, and with the functional coefficients

$$ \begin{aligned} \alpha^{\pm}_{(lm)}(\theta) &= \frac{2m^2 - l(l+1)}{\sin^2\theta} \mp 2m(l-1)\frac{\cot\theta}{\sin\theta} + l(l-1)\cot^2\theta \\ \beta^{\pm}_{(lm)}(\theta) &= 2\left[\frac{2l+1}{2l-1}\left(l^2-m^2\right)\right]^{1/2}\left(\pm\frac{m}{\sin^2\theta} + \frac{\cot\theta}{\sin\theta}\right). \end{aligned} \tag{15} $$

This relation holds once more under the convention that Y_{lm} is defined to be zero for $l < |m|$.

Consequently, the direct spin-weighted spherical harmonics transform of a spin ± 2 function ${}_{\pm 2}G$ may be written as a linear combination of direct scalar spherical harmonics transforms for three associated scalar functions. Indeed, if the associated functions are defined by $G^{(p)}(\theta,\varphi) = (\cot^p\theta/\sin^q\theta)\,{}_{\pm 2}G(\theta,\varphi)$, for $p, q \in \mathbb{N}$ and $p+q=2$, one gets from relation (14):

$$ \begin{aligned} {}_{\pm 2}\widehat{G}_{lm} = \left[\frac{(l-2)!}{(l+2)!}\right]^{1/2} \Bigg\{ & 2\left[\frac{2l+1}{2l-1}\left(l^2-m^2\right)\right]^{1/2}\left(\widehat{G^{(1)}}_{(l-1)m} \pm m\widehat{G^{(0)}}_{(l-1)m}\right) \\ & + l(l-1)\,\widehat{G^{(2)}}_{lm} \mp 2m(l-1)\,\widehat{G^{(1)}}_{lm} + \left[2m^2 - l(l+1)\right]\widehat{G^{(0)}}_{lm}\Bigg\}, \end{aligned} \tag{16} $$

with $l \geq 2$ and $|m| \leq l$. The relation (14) also implies that the inverse spin-weighted transform of a set of spin ± 2 coefficients ${}_{\pm 2}\widehat{G}_{lm}$ (with ${}_{\pm 2}\widehat{G}_{lm} = 0$ for $l \geq L$) may be written as a sum of three inverse scalar spherical harmonics transforms:

$$ G(\theta,\varphi) = \frac{1}{\sin^2\theta}A(\theta,\varphi) + \frac{\cot\theta}{\sin\theta}B(\theta,\varphi) + \cot^2\theta\, C(\theta,\varphi), \tag{17} $$

with the scalar functions A, B, and C identified as follows by their scalar spherical harmonics coefficients:

$$
\begin{aligned}
\widehat{A}_{lm} &= \left[\frac{(l-2)!}{(l+2)!}\right]^{1/2} \left[2m^2 - l\,(l+1)\right] {}_{\pm 2}\widehat{G}_{lm} \\
&\quad \pm 2m \left[\frac{(l-1)!}{(l+3)!}\frac{(2l+3)}{(2l+1)}\left((l+1)^2 - m^2\right)\right]^{1/2} {}_{\pm 2}\widehat{G}_{(l+1)m} \\
\widehat{B}_{lm} &= \left[\frac{(l-2)!}{(l+2)!}\right]^{1/2} \left[\mp 2m\,(l-1)\right] {}_{\pm 2}\widehat{G}_{lm} \\
&\quad + 2 \left[\frac{(l-1)!}{(l+3)!}\frac{(2l+3)}{(2l+1)}\left((l+1)^2 - m^2\right)\right]^{1/2} {}_{\pm 2}\widehat{G}_{(l+1)m} \\
\widehat{C}_{lm} &= \left[\frac{(l-2)!}{(l+2)!}\right]^{1/2} \left[l\,(l-1)\right] {}_{\pm 2}\widehat{G}_{lm}.
\end{aligned} \tag{18}
$$

As discussed, for functions band-limited at L, the separation of variables allows to compute the direct and inverse scalar spherical harmonics transforms in $\mathcal{O}(L^3)$ operations. However, a faster algorithm was developed by Driscoll and Healy on $2L \times 2L$ equi-angular pixelizations on the sphere for the scalar spherical harmonics transforms [23]. The Fourier transforms in $e^{im\varphi}$ are computed in $\mathcal{O}(L \log_2 L)$ operations for each θ through standard Cooley-Tukey fast Fourier transforms. The algorithm also explicitly takes advantage of the recurrence relation in l on the associated Legendre polynomials $P_l^m(\cos\theta)$ to compute the direct associated Legendre transforms in $\mathcal{O}(L \log_2^2 L)$ operations for each m. In these terms, the direct and inverse scalar spherical harmonics transforms are computed in $\mathcal{O}(L^2 \log_2^2 L)$ operations. The computation is theoretically exact thanks to the sampling theorem on equi-angular pixelizations. Corresponding stable numerical implementations exist in the SpharmonicKit package [25,26] [3]. Through the relations (16) and (17), the spin-weighted spherical harmonics transform of a band-limited spin ± 2 function with band limit L may consequently also be computed exactly on a $2L \times 2L$ equi-angular pixelization on the sphere from the Driscoll and Healy fast scalar spherical harmonics transforms, and with the same asymptotic complexity of order $\mathcal{O}(L^2 \log_2^2 L)$. In terms of our previous intuitive estimations, we recall that an $\mathcal{O}(L^2)$ scalar product requires the order of 0.03 seconds on a standard 2.2 GHz Intel Pentium Xeon CPU, at band limits around $L \simeq 10^3$. When compared to the *a priori* $\mathcal{O}(L^4)$ asymptotic complexity, the $\mathcal{O}(L^2 \log_2^2 L)$ scalar and spin ± 2 spherical harmonics transforms algorithms consequently reduce computation times from days to seconds for the fine samplings considered.

Let us remark that a recurrence relation was proposed in [27] in order to compute spin n spherical harmonics transforms from scalar spherical harmonics transforms. However, the proposed relation explicitly relates ${}_nY_{lm}$ with ${}_{n\mp 1}Y_{lm}$, ${}_{n\mp 1}Y_{(l-1)m}$, and ${}_{n\mp 1}Y_{(l+1)m}$. The term ${}_{n\mp 1}Y_{(l+1)m}$ increases the band limit of the functions to be analyzed to $L+2$ after the 2-steps recurrence leading from

[3] http://www.cs.dartmouth.edu/∼geelong/sphere/

spin ± 2 to scalar spherical harmonics. On $2L \times 2L$ equi-angular pixelizations, the SpharmonicKit package is technically limited to consider coefficients lower than L, and numerical errors will occur due to the absence of consideration of the coefficients at $l = L$ and $l = L + 1$. No such issue occurs from the relation (14) here above, which preserves the band limit L for the associated scalar functions.

3.3 Numerical implementation

We here report the computation times and memory requirements for the numerical implementation of the algorithm at band limits up to $L = 1024$, and briefly discuss the issue of the numerical stability of the implementation. The implementation is directly based on the fast scalar spherical harmonics transform proposed by Driscoll and Healy and implemented in the SpharmonicKit package. Computations are performed on a 2.20 GHz Intel Pentium Xeon CPU with 2 Gb of RAM memory. Random band-limited test-functions are considered. Without loss of generality, these test-functions are defined through their spin-weighted spherical harmonics coefficients ${}_{\pm 2}\widehat{G}_{lm}$, with $|m| \leq l < L$, and $l \geq 2$, with independent real and imaginary parts uniformly distributed in the interval $[-1, +1]$. The inverse and direct spin-weighted spherical harmonics transforms are successively computed, giving numerical coefficients ${}_{n}\widehat{H}_{lm}$.

The computation times given in Table 1 for the direct and inverse spin ± 2 transforms are averages over 5 random test-functions. They range between 1.0×10^{-1} seconds for $L = 128$ and 2.2×10^{1} seconds for $L = 1024$. The equality of computation times for the positive and negative spins is an evident consequence of the similarity of the ± 2 cases in the relation (14). The case $n = 0$ corresponds to the scalar spherical harmonics transform, and is added for comparison. The related values range between 2.7×10^{-2} seconds for $L = 128$ and 6.5 seconds for $L = 1024$. To summarize, computation times are of the order of seconds for a band limit $L = 1024$, in agreement with our previous intuitive estimations. Both for the direct and inverse transforms, the evolution of the values reported as a function of the band limit also supports the $\mathcal{O}(L^2 \log_2^2 L)$ behavior of the related asymptotic complexity, as illustrated in figure 1 in comparison with an $\mathcal{O}(L^3)$ slope. The ratio of computation times for the cases $n = \pm 2$ and $n = 0$ also reflects the simple fact that three scalar transforms are computed for each spin ± 2 transform.

In the present implementation based on the SpharmonicKit package, the required associated Legendre polynomials $P_l^m(\cos\theta)$ are pre-calculated once for all values of l, θ, and m, and stored in RAM memory. The pre-computation time itself is of order $\mathcal{O}(L^3)$ through the use of a recurrence relation in l on the associated Legendre polynomials. This pre-computation is by definition

Spin	Time $L = 128$ (sec)	Time $L = 256$ (sec)	Time $L = 512$ (sec)	Time $L = 1024$ (sec)
$n = 0$	$3.7\text{e}-02$	$2.0\text{e}-01$	$1.1\text{e}+00$	$6.5\text{e}+00$
	$2.7\text{e}-02$	$1.4\text{e}-01$	$8.1\text{e}-01$	$6.2\text{e}+00$
$n = 2$	$1.2\text{e}-01$	$6.4\text{e}-01$	$3.6\text{e}+00$	$2.2\text{e}+01$
	$1.0\text{e}-01$	$5.0\text{e}-01$	$2.9\text{e}+00$	$2.1\text{e}+01$
$n = -2$	$1.2\text{e}-01$	$6.4\text{e}-01$	$3.5\text{e}+00$	$2.1\text{e}+01$
	$1.0\text{e}-01$	$5.0\text{e}-01$	$2.9\text{e}+00$	$2.1\text{e}+01$

Table 1
Computation times for $n = 0$ and $n = \pm 2$ spherical harmonics transforms measured on a 2.20 GHz Intel Pentium Xeon CPU with 2 Gb of RAM memory. Times associated with the direct transforms are listed above the corresponding times for the inverse transforms.

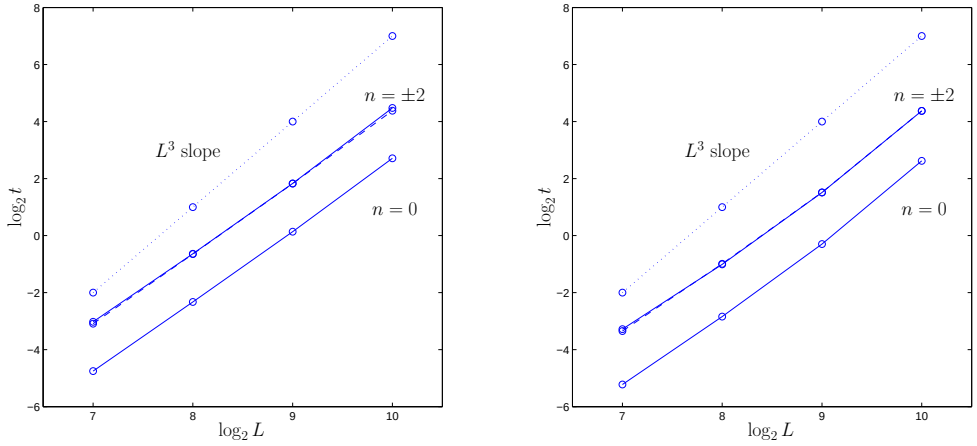

Figure 1. Evolution of computation times t displayed as $\log_2 t - \log_2 L$ for the direct (left) and inverse (right) spin-weighted spherical harmonics transforms of spins $n = 0$ (continuous line), $n = +2$ (continuous line), and $n = -2$ (dashed line). Computation times are measured in seconds on a 2.20 GHz Intel Pentium Xeon CPU with 2 Gb of RAM memory, and reported for the band limits $L \in \{128, 256, 512, 1024\}$. The $\mathcal{O}(L^2 \log^2 L)$ asymptotic complexity is clearly illustrated when compared to an $\mathcal{O}(L^3)$ slope (dotted line).

not taken into account in the reported computation times, which consequently remain of order $\mathcal{O}(L^2 \log_2^2 L)$. The number of real values of associated Legendre polynomials $P_l^m(\cos\theta)$ stored in RAM memory for all l, θ, and m is also of order $\mathcal{O}(L^3)$. The overall memory requirements allowing the direct and inverse transforms with the present numerical implementation correspondingly increase from 5.6 Mb for $L = 128$, to 32 Mb for $L = 256$, 220 Mb for $L = 512$, and 1.2 Gb for $L = 1024$. These memory requirements are easily accessible on a single standard computer.

Spin	Error $L = 128$	Error $L = 256$	Error $L = 512$	Error $L = 1024$
$n = 0$	$1.8\text{e}-10$	$6.5\text{e}-10$	$2.3\text{e}-09$	$8.4\text{e}-09$
	$9.7\text{e}-10$	$5.7\text{e}-09$	$1.6\text{e}-08$	$1.1\text{e}-07$
$n = 2$	$1.8\text{e}-10$	$6.6\text{e}-10$	$2.4\text{e}-09$	$8.3\text{e}-09$
	$7.2\text{e}-10$	$4.2\text{e}-09$	$4.6\text{e}-08$	$4.2\text{e}-07$
$n = -2$	$1.8\text{e}-10$	$6.6\text{e}-10$	$2.3\text{e}-09$	$8.3\text{e}-09$
	$9.8\text{e}-10$	$2.9\text{e}-09$	$3.1\text{e}-08$	$1.2\text{e}-07$

Table 2
Errors are measured on a 2.20 GHz Intel Pentium Xeon CPU with 2 Gb of RAM memory. Absolute errors after inverse and direct transforms are listed above the corresponding relative errors.

The absolute and relative numerical errors are defined as $\max_{l,m} |\ {}_n\widehat{G}_{lm} - {}_n\widehat{H}_{lm}|$ and $\max_{l,m} |(\ {}_n\widehat{G}_{lm} - \ {}_n\widehat{H}_{lm})/\ {}_n\widehat{G}_{lm}|$ respectively, where $|\cdot|$ here denotes the complex norm, and $n \in \{0, \pm 2\}$. The numerical errors associated with the $\mathcal{O}(L^2 \log_2^2 L)$ spin-weighted spherical harmonics transforms given in Table 2 are averages for transforms over 5 random band-limited test-functions. Absolute and relative errors do not exceed the order of 8.4×10^{-9} and 4.2×10^{-7} respectively for band limits up to $L = 1024$. The $\mathcal{O}(L^2 \log_2^2 L)$ implementation of the spin ± 2 spherical harmonics transforms is therefore stable for band limits up to $L = 1024$. The numerical stability of the algorithm might also have been inferred from the corresponding stability of the Driscoll and Healy fast direct scalar spherical harmonics transform algorithm, tested for band limits up to $L = 1024$ [25,26]. The only potential source of instability is related to the multiplication factor $\cot^p \theta / \sin^q \theta$ defining the scalar functions associated with a spin ± 2 function in the computation of a spin-weighted spherical harmonics transform from the relation (14). Each such factor indeed corresponds to a division by $\sin^2 \theta$, which induces multiplications by numbers of the order of L^2 around the poles $\theta = \{0, \pi\}$, where L is the band limit considered. However such operations could only produce numerical instabilities for very high band limits, and obviously remain completely safe at $L = 1024$.

4 Application in cosmology

In this section, we illustrate the interest of the algorithm presented in the previous section in the context of the analysis of CMB polarization data. The discussion is based on the following introductory papers [5,6,7,8,9,10] and reviews [28,29,30,31] relative to the CMB polarization analysis.

4.1 Stokes parameters

The CMB is observed in each direction $\omega = (\theta, \varphi)$ of the sky as an incoming radial radiation, to which is associated a transverse electromagnetic field thus lying in the tangent plane to the sphere at the point considered. In that plane, we consider the basis $(\hat{e}_\theta, \hat{e}_\varphi)$ with $\hat{e}_\theta$ pointing in the direction of increasing θ along each meridian, and $\hat{e}_\varphi$ in the direction of increasing φ along each parallel. In this so-called linear polarization basis, nearly monochromatic radiation around a frequency ω_r may be decomposed as an electric field with components $E_\theta(\omega_r, t) = \mathcal{R}e[\varepsilon_\theta(t)e^{-i\omega_r t}]$ and $E_\varphi(\omega_r, t) = \mathcal{R}e[\varepsilon_\varphi(t)e^{-i\omega_r t}]$. The complex amplitudes $\varepsilon_\theta(t)$ and $\varepsilon_\varphi(t)$ slowly vary in time relatively to the timescale set by the wave period. The intensity matrix $\mathbf{I}$ associated with the radiation simply reads as the time average of the electric field rank 2 tensor $[\varepsilon_i^*(t)\varepsilon_j(t)]\hat{e}_i \otimes \hat{e}_j$, for $i, j \in \{\theta, \varphi\}$ [5,10]. It thus naturally decomposes on the 2×2 matrix basis formed by the identity matrix $\sigma_0 = \mathbb{I}$, and the well-known Pauli matrices $(\sigma_1, \sigma_2, \sigma_3)$, as $\mathbf{I} = [I\sigma_0 + U\sigma_1 + V\sigma_2 + Q\sigma_3]/2$. The constants I, U, V, and Q define the four real Stokes parameters [32] associated with the radiation: $I = \langle|\varepsilon_\theta(t)|^2 + |\varepsilon_\varphi(t)|^2\rangle$, $Q = \langle|\varepsilon_\theta(t)|^2 - |\varepsilon_\varphi(t)|^2\rangle$, $U = \langle\varepsilon_\theta^*(t)\varepsilon_\varphi(t) + \varepsilon_\theta(t)\varepsilon_\varphi^*(t)\rangle$, $V = i\langle\varepsilon_\theta^*(t)\varepsilon_\varphi(t) - \varepsilon_\theta(t)\varepsilon_\varphi^*(t)\rangle$. The brackets $\langle\cdot\rangle$ denote time averaging. If the two components $\varepsilon_\theta(t)$ and $\varepsilon_\varphi(t)$ are correlated, the radiation is said to be polarized. The positive parameter I may be identified with the overall intensity of radiation, while Q and U identify with the linear polarizations, and V with the circular polarization. Unpolarized radiation, or natural light, is therefore characterized by $Q = U = V = 0$.

As functions on the sphere, $I(\omega)$, $Q(\omega)$, $U(\omega)$ and $V(\omega)$ have different behaviors both under parity, *i.e.* global inversion $(\cdot'')$ of the coordinates, and under local rotations $(\cdot')$ of the basis vectors $(\hat{e}_\theta, \hat{e}_\varphi)$ in the tangent plane at $\omega = (\theta, \varphi)$. A global inversion of the right-handed three-dimensional Cartesian coordinate system $(o, o\hat{x}, o\hat{y}, o\hat{z})$ centered on the unit sphere induces the following modification of Cartesian coordinates: $(x'', y'', z'') = (-x, -y, -z)$. The spherical coordinates $\omega = (\theta, \varphi)$ of a given point on S^2 change according to $\omega'' = (\theta'', \varphi'') = (\pi - \theta, \pi + \varphi)$. Locally in the tangent plane, the global inversion also implies an inversion of the basis vector $\hat{e}_\theta$: $(\hat{e}''_\theta, \hat{e}''_\varphi) = (-\hat{e}_\theta, \hat{e}_\varphi)$. The Stokes parameters I and Q have even parity, $I''(\omega'') = I(\omega)$ and $Q''(\omega'') = Q(\omega)$, while U and V have odd parity, $U''(\omega'') = -U(\omega)$ and $V''(\omega'') = -V(\omega)$. Under local rotations of the basis vectors $(\hat{e}_\theta, \hat{e}_\varphi)$ by an angle χ_0, the coordinates $\vec{\varepsilon} = (\varepsilon_\theta, \varepsilon_\varphi)$ of vectors in the tangent plane transform through $\vec{\varepsilon}' = r_{\chi_0} \cdot \vec{\varepsilon}$, for the standard rotation matrix r_{χ_0}, with entries $r^{11}_{\chi_0} = r^{22}_{\chi_0} = \cos\chi_0$ and $r^{12}_{\chi_0} = -r^{21}_{\chi_0} = \sin\chi_0$. The Stokes parameters I and V are invariant while Q and U are mixed by local rotations. Equivalently, one may also rewrite the intensity matrix as

$$\mathbf{I} = \frac{1}{2}\left[I\sigma_0 + V\sigma_2 + (Q + iU)\,\sigma_+ + (Q - iU)\,\sigma_-\right], \tag{19}$$

with $\sigma_\pm = (\sigma_3 \mp i\sigma_1)/2$. The Pauli matrices transform as $\sigma'_\mu = r_{\chi_0} \cdot \sigma_\mu \cdot r^T_{\chi_0}$, for $\mu = \{0, 1, 2, 3\}$. The matrices σ_0 and σ_2 are thus invariant, while $\sigma_\pm$ transform as $\sigma'_\pm = e^{\mp 2i\chi_0}\sigma_\pm$. Consequently the four Stokes parameters are associated with spin functions on the sphere. The intensity $I(\omega)$ and the circular polarization parameter $V(\omega)$ are scalar functions. The combinations $(Q \pm iU)(\omega)$ are spin ± 2 functions: $(Q \pm iU)'(\omega) = e^{\mp 2i\chi_0}(Q \pm iU)(\omega)$. Notice that under parity these two combinations transform in one another: $(Q \pm iU)''(\omega'') = (Q \mp iU)(\omega)$ [6,10].

4.2 Angular power spectra

It is assumed that the physics of the CMB is invariant under parity and under local rotations. It is therefore suitable to relate the observables I, Q, U, and V to invariant physical quantities. The intensity $I(\omega)$ defines the CMB temperature anisotropies $T(\omega)$ and is indeed itself invariant under the transformations considered. As no circular polarization may arise from Thomson scattering, the CMB polarization is completely described in terms of the two linear polarization Stokes parameters Q and U. It is equivalently defined by their spin ± 2 combinations $Q \pm iU$. Associated polarization components, real scalar functions on the sphere and parity eigenmodes, are naturally defined from $Q \pm iU$ in terms of the raising $\eth$ and lowering $\bar{\eth}$ operators respectively given in (5) and (6). These components $\tilde{E}(\omega) = -[\bar{\eth}^2(Q + iU)(\omega) + \eth^2(Q - iU)(\omega)]/2$, and $\tilde{B}(\omega) = i[\bar{\eth}^2(Q + iU)(\omega) - \eth^2(Q - iU)(\omega)]/2$, have even and odd parities and are therefore referred to as electric and magnetic components respectively [6]. Let us consider the decomposition of the spin ± 2 functions $Q \pm iU$ in spin-weighted spherical harmonics and the relations ${}_2Y_{lm} = N_{(l2)}\eth^2 Y_{lm}$ and ${}_{-2}Y_{lm} = N_{(l2)}\bar{\eth}^2 Y_{lm}$, with $N_{(l2)} = [(l-2)!/(l+2)!]^{1/2}$, induced from (10) and (11). The application of the raising and lowering operators on this decomposition through the relations (7) to (9) gives $\hat{\tilde{E}}_{lm} = \hat{E}_{lm}/N_{(l2)}$ and $\hat{\tilde{B}}_{lm} = \hat{B}_{lm}/N_{(l2)}$, where

$$\hat{E}_{lm} = -\frac{1}{2}\left({}_{+2}\widehat{(Q + iU)}_{lm} + {}_{-2}\widehat{(Q - iU)}_{lm}\right) \tag{20}$$

and

$$\hat{B}_{lm} = \frac{i}{2}\left({}_{+2}\widehat{(Q + iU)}_{lm} - {}_{-2}\widehat{(Q - iU)}_{lm}\right), \tag{21}$$

define the properly normalized real $E(\omega)$ and $B(\omega)$ components. These coefficients are explicitly invariant under local rotations.

The random process from which the CMB radiation arises is assumed to be Gaussian and stationary. It is therefore completely characterized in terms of its temperature and polarization two-point correlation functions. The corresponding invariant angular power spectra are naturally those associated with the

temperature TT, the polarizations EE and BB, and the cross-correlation between the temperature and electric polarization component TE: $\langle \widehat{T}^*_{l'm'} \widehat{T}_{lm} \rangle = C_l^{TT} \delta_{ll'} \delta_{mm'}$, $\langle \widehat{E}^*_{l'm'} \widehat{E}_{lm} \rangle = C_l^{EE} \delta_{ll'} \delta_{mm'}$, $\langle \widehat{B}^*_{l'm'} \widehat{B}_{lm} \rangle = C_l^{BB} \delta_{ll'} \delta_{mm'}$, $\langle \widehat{T}^*_{l'm'} \widehat{E}_{lm} \rangle = C_l^{TE} \delta_{ll'} \delta_{mm'}$. These physical quantities are indeed invariant under local rotations and parity. The TB and EB cross-correlations are specifically excluded from the requirement of invariance under parity.

Notice that the E and B components of polarization not only define invariant physical angular power spectra, but they are also associated with different mechanisms of production of the radiation, corresponding to different theoretical cosmological models. Scalar primordial energy density perturbations only produce the E polarization component, while vector and tensor (*i.e.* gravity waves) perturbations produce both E and B polarization components.

4.3 Numerical illustration

Scalar and spin ± 2 direct spherical harmonics transforms are required for the estimation of the CMB angular power spectra from the observables T, Q, and U [6]. The simulation of temperature and polarization maps from given theoretical angular power spectra requires the corresponding inverse transforms. We apply our algorithm to simulate CMB maps and angular power spectra, for illustration of its precision and speed performances.

We start from the temperature and polarization spectra C_l^{TT}, C_l^{EE}, and C_l^{TE} defined by the concordance cosmological model which best fits the three-year WMAP data (the BB polarization spectrum is identically null: $C_l^{BB} = 0$). These spectra are represented in figure 2 up to a band limit $L = 1024$. Spherical harmonics coefficients $\widehat{T}_{lm}$ and $\widehat{E}_{lm}$ are built up as the two marginal complex Gaussian realizations arising from a jointly Gaussian statistical distribution with variances C_l^{TT} and C_l^{EE}, and a covariance C_l^{TE}. The T, Q, and U maps are then produced by inverse scalar and spin ± 2 transforms, through the relations (20) and (21), with $\widehat{B}_{lm} = 0$.

From the maps obtained, we recompute spherical harmonics coefficients $\widehat{T}'_{lm}$, $\widehat{E}'_{lm}$, and $\widehat{B}'_{lm}$ by direct scalar and spin ± 2 transforms. Within the numerical accuracy of the computer, the B polarization coefficients are identically null, in perfect agreement with the original data: $\widehat{B}'_{lm} = 0$. We finally estimate the temperature and polarization angular power spectra from those coefficients as: $C_l^{TT\prime} = \sum_{m=-l}^{l} |\widehat{T}'_{lm}|^2/(2l+1)$, $C_l^{EE\prime} = \sum_{m=-l}^{l} |\widehat{E}'_{lm}|^2/(2l+1)$, $C_l^{TE\prime} = \sum_{m=-l}^{l} \widehat{T}'^*_{lm} \widehat{E}'_{lm}/(2l+1)$, and $C_l^{BB\prime} = \sum_{m=-l}^{l} |\widehat{B}'_{lm}|^2/(2l+1) = 0$. These estimators follow chi-square distributions with $2l+1$ degrees of freedom. For $X \in \{TT, EE, BB, TE\}$, this induces a fractional uncertainty $\sigma_{C_l^{X\prime}}/C_l^X = [2/(2l+1)]^{1/2}$ in the estimation. This cosmic variance is large at low l and

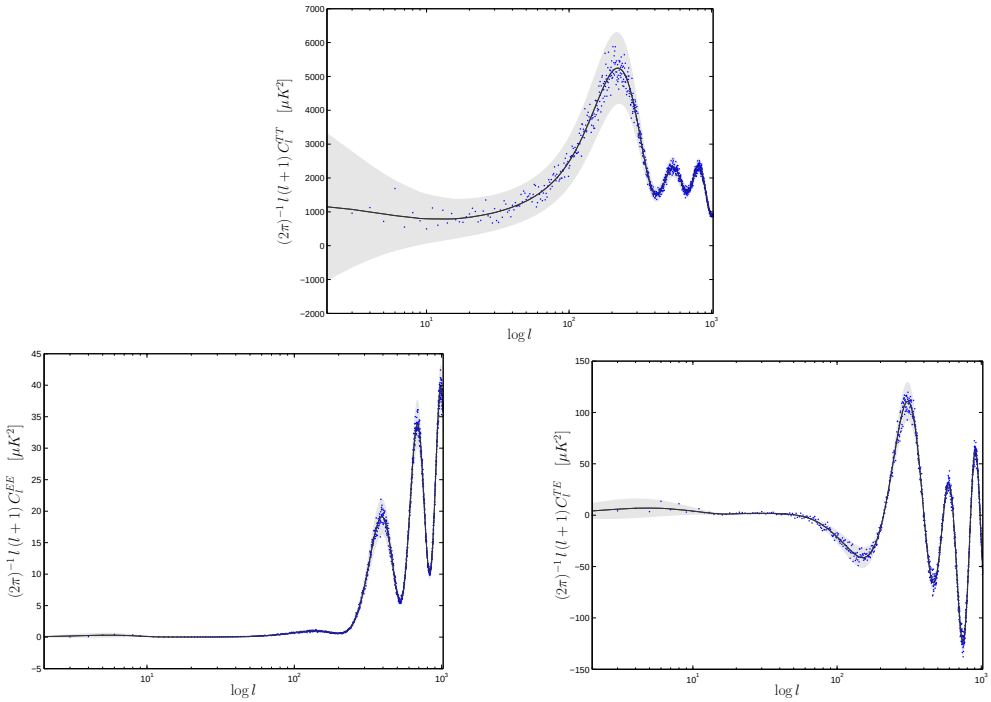

Figure 2. CMB temperature and polarization angular power spectra C_l^{TT} (top), C_l^{EE}(bottom left), and C_l^{TE} (bottom right) of the cosmic microwave background up to a band limit $L = 1024$ and in μK^2. Inverse and direct transforms are successively performed through the exact $\mathcal{O}(L^2 \log_2^2 L)$ scalar and spin ± 2 spherical harmonics transforms on $2L \times 2L$ equi-angular pixelizations on the sphere, in order to produce the estimated spectra (scattered points) from the original spectra of the concordance cosmological model (continuous lines). The original and estimated spectra coincide within the 3σ uncertainty defined by the cosmic variance (grey region).

small at high l. The figure 2 represents the good coincidence between the original and estimated spectra up to the corresponding uncertainty at each l. The computation time associated with the overall procedure is 150 seconds on a 2.20 GHz Intel Pentium Xeon CPU with 2 Gb of RAM memory. In summary, this application illustrates the good precision and speed performances of our fast and exact algorithm, coherently with the results of tables 1 and 2.

5 Conclusion

In conclusion, we developed a fast, exact, and stable algorithm for the spin ± 2 spherical harmonics transforms of band-limited functions with band limit L on $2L \times 2L$ equi-angular pixelizations on the sphere. The algorithm is based the Driscoll and Healy fast scalar spherical harmonics transform algorithm. The exactness of the computation on equi-angular pixelizations relies on a sampling theorem. The associated asymptotic complexity is of order $\mathcal{O}(L^2 \log_2^2 L)$. The algorithm is presented as an alternative to existing algorithms with an asymp-

totic complexity of order $\mathcal{O}(L^3)$ on the HEALPix and GLESP pixelizations, which are widely used in the context of astrophysics and cosmology.

The numerical implementation produced confirms the characteristics of the algorithm. Typical computation times for $L = 1024$ are of the order of seconds. We also illustrated the interest of the algorithm in the context of the analysis of CMB polarization data.

Acknowledgements

The authors wish to thank P. Vielva, J.-P. Antoine, B. Barreiro, and E. Martínez-González for valuable comments and discussions. Y. W. acknowledges support of the Swiss National Science Foundation (SNF) under contract No. 200021-107478/1. He is also postdoctoral researcher of the Belgian National Science Foundation (FRS-FNRS). L. J. is postdoctoral researcher of the Belgian National Science Foundation (FRS-FNRS).

References

[1] C. L. Bennett *et al.*, Astrophys. J. Suppl. **148**, 1 (2007).

[2] G. Hinshaw *et al.*, Astrophys. J. Suppl. **170**, 288 (2007).

[3] D. N. Spergel *et al.*, Astrophys. J. Suppl. **148**, 175 (2003).

[4] D. N. Spergel *et al.*, Astrophys. J. Suppl. **170**, 377 (2007).

[5] A. Kosowsky, Ann. Phys. **246**, 49 (1996).

[6] M. Zaldarriaga and U. Seljak, Phys. Rev. D **55**, 1830 (1997).

[7] U. Seljak and M. Zaldarriaga, Phys. Rev. Lett. **78**, 2054 (1997).

[8] M. Kamionkowski, A. Kosowsky, and A. Stebbins, Phys. Rev. Lett. **78**, 2058 (1997).

[9] M. Kamionkowski, A. Kosowsky, and A. Stebbins, Phys. Rev. D **55**, 7368 (1997).

[10] W. Hu and M. White, Phys. Rev. D **56**, 596 (1997).

[11] L. Page *et al.*, Astrophys. J. Suppl. **170**, 335 (2007).

[12] D. A. Varshalovich, A. N. Moskalev, and V. K. Khersonskii, *Quantum Theory of Angular Momentum*, First Edition Reprint, World Scientific, Singapore (1989).

[13] M. Abramowitz and I. Stegun, *Handbook of mathematical functions*, Dover Publications Inc., New York (1965).

[14] D. M. Brink and G. R. Satchler, *Angular Momentum*, Third Edition, Clarendon Press, Oxford (1993).

[15] E. T. Newman and R. Penrose, J. Math. Phys. **7**, 863 (1966).

[16] J. N. Goldberg, A. J. Macfarlane, E. T. Newman, F. Rohrlich, and E. C. G. Sudarshan, J. Math. Phys. **8**, 2155 (1967).

[17] M. Carmeli, J. Math. Phys. **10**, 569 (1969).

[18] K. M. Górski, E. Hivon, A. J. Banday, B. D. Wandelt, F. K. Hansen, M. Reinecke, and M. Bartelman, Astrophys. J. **622**, 759 (2005).

[19] A. G. Doroshkevich, P. D. Naselsky, O. V. Verkhodanov, D. I. Novikov, V. I. Turchaninov, I. D. Novikov, P. R. Christensen, and L.-Y. Chiang, Int. J. Mod. Phys. D **14**, 275 (2005).

[20] A. G. Doroshkevich, P. D. Naselsky, O. V. Verkhodanov, D. I. Novikov, V. I. Turchaninov, I. D. Novikov, P. R. Christensen, and L.-Y. Chiang, preprint astro-ph/0501494 (2005).

[21] D. K. Maslen and D. N. Rockmore, J. American Math. Soc. **10**, 169 (1997).

[22] D. K. Maslen and D. N. Rockmore, in Proc. DIMACS Workshop on Groups and Computation 28, ed. L. Finkelstein and W. Kantor, American Math. Soc., Providence, 183 (1997).

[23] J. R. Driscoll and D. M. Healy Jr., Adv. in Appl. Math. **15**, 202 (1994).

[24] Y. Wiaux, L. Jacques, P. Vielva, and P. Vandergheynst, Astrophys. J. **652**, 820 (2006).

[25] D. M. Healy Jr., D. N. Rockmore, P. J. Kostelec, and S. Moore, J. Fourier Anal. and Applic. **9**, 341 (2003).

[26] D. M. Healy Jr., P. J. Kostelec, and D. N. Rockmore, Adv. in Comput. Math. **21**, 59 (2004).

[27] P. J. Kostelec, D. K. Maslen, D. N. Rockmore, and D. M. Healy Jr., J. Comput. Phys. **162**, 514 (2000).

[28] W. Hu and M. White, New A **2**, 323 (1997).

[29] A. Kosowsky, New A Rev. **43**, 157 (1999).

[30] P. Cabella and M. Kamionkowski, preprint astro-ph/0403392 (2004).

[31] Y.-T. Lin and B. D. Wandelt, Astropart. Phys. **25**, 151 (2006).

[32] J. D. Jackson, *Classical Electromagnetism*, Second Edition, J. Wiley & Sons Inc., New York (1975).